



HAL
open science

New fluorinated polymer- based nanocomposites via combination of sol -gel chemistry and reactive extrusion for polymer electrolyte membranes fuel cells (PEMFCs)

Sérigne Seck, Sylvain Magana, Arnaud Prébé, Pierrick Buvat, Janick Bigarré, Jérôme Chauveau, Bruno Ameduri, Jean-François Gérard, Véronique Bounor-Legaré

► To cite this version:

Sérigne Seck, Sylvain Magana, Arnaud Prébé, Pierrick Buvat, Janick Bigarré, et al.. New fluorinated polymer- based nanocomposites via combination of sol -gel chemistry and reactive extrusion for polymer electrolyte membranes fuel cells (PEMFCs). *Materials Chemistry and Physics*, 2020, 252, pp.123004. 10.1016/j.matchemphys.2020.123004 . hal-02798995

HAL Id: hal-02798995

<https://hal.science/hal-02798995>

Submitted on 17 Dec 2020

HAL is a multi-disciplinary open access archive for the deposit and dissemination of scientific research documents, whether they are published or not. The documents may come from teaching and research institutions in France or abroad, or from public or private research centers.

L'archive ouverte pluridisciplinaire **HAL**, est destinée au dépôt et à la diffusion de documents scientifiques de niveau recherche, publiés ou non, émanant des établissements d'enseignement et de recherche français ou étrangers, des laboratoires publics ou privés.

New fluorinated polymer-nanocomposites based via combination of sol -gel chemistry and reactive extrusion for Polymer Electrolyte Membranes Fuel Cells (PEMFC)

Serigne Seck^{1,2}, Sylvain Magana¹, Arnaud Prébé^{1,2}, Pierrick Buvat³, Janick Bigarré³, Jérôme Chauveau⁴, Bruno Améduri⁵, Jean-François Gérard², Véronique Bounor-Legaré^{1,*}

(1) Univ Lyon, Université Lyon1, UMR CNRS 5223, Ingénierie des Matériaux Polymères, F-69622, LYON, France

(2) Univ Lyon, INSA de Lyon, CNRS UMR 5223, Ingénierie des Matériaux Polymères, F-69621, LYON, France

(3)CEA-DAM – LSTP - Centre Le Ripault – F-37260 Monts, France

(4) ARKEMA - CERDATO - Route de Launay - F-27470 Serquigny France

(5) IAM-Institut Charles Gerhardt - UMR 5253- CNRS, UM, ENSCM-

Place Eugène Bataillon - F-34296 Montpellier Cedex, France

*E-mail: bounor@univ-lyon1.fr

Abstract

Proton exchange membranes designed via reactive extrusion from the *in situ* generation of functional silica-like particles in a new poly(vinylidene fluoride-*co*-hexafluoropropylene (poly(VDF-*co*-HFP)) copolymer are presented. These sulfonic acid-functionalized polysiloxane-based fillers were synthesized *via* sol-gel chemistry from 3-mercaptopropyltri(ethoxy)silane and polydimethoxysiloxane in the molten PVDF-*co*-HFP polymer. To process such nanocomposites materials, the reactive extrusion parameters were selected to (i) reach silanol condensation extents in the processing conditions of a

conventional poly(VDF-*co*-HFP) copolymer and (ii) obtain a surface functionalization high enough with respect to reach a suitable protonic conductivity value of the nanocomposites films. Nevertheless, the enhancement of the proton conductivity being deeply associated with the morphologies of the nanocomposites materials (i.e. the dispersed functional silica phase need to display the larger interface area with the polymer matrix), an interfacial agent was synthesized. This compatibilizer was either poly(VDF-*co*- α -trifluoromethacrylic acid) or poly(VDF-*co*-MAF) copolymers or a poly(VDF-*co*-HFP) copolymer grafted with maleic anhydride, denoted poly(VDF-*co*-HFP)-*g*-MA. In a second step, to obtain the required sulfonic acid-functionalized silica dispersed phase from the presence of the mercaptan functions, the resulting films were oxidized. Electrochemical properties were evaluated: for a theoretical ionic exchange capacity (IEC) of 2 meq.g⁻¹, while experimental IEC ranged between 1.0 and 1.3 meq.g⁻¹. The proton conductivity was found to reach 78 mS.cm⁻¹ at room temperature for 100% of relative humidity. Interestingly, these values are higher than those of the same membranes processed without any compatibilizer (54 mS.cm⁻¹) and to that of Nafion[®] NR112 (52 mS.cm⁻¹). This approach also allows limiting the swelling (or water uptake) of proton conductive membranes below 15wt% while it reaches 30 wt% for Nafion[®] NR112 in similar conditions.

Keywords: energy; fluoropolymers; fluorinated nanocomposites; PEMFC proton conductivity; reactive processing; sol-gel.

1 Introduction

Environmental protection is a major societal concern. Fossil fuel consumption is not only the major current source of pollution and environmental degradation, but petrosourced resources are also becoming more expensive and a drag on the world economy. The development of alternative clean-energy technologies has therefore become a key requirement for sustainable long-term development [1-4]. The increased energy density required to promote this tomorrow revolution implies the development of ‘new’ chemistries for fuel cells, lithium-ion batteries, and for photovoltaic- and ferro- or piezoelectric devices [5-9]. Fluoropolymers [10-13] are suitable candidates to fulfill the various stringent requirements for these technologies known by their remarkable thermal, chemical, electrochemical, and mechanical properties and have widely been used as polymer electrolytes for proton exchange membranes for fuel cells (PEMFCs). Currently, perfluorosulfonic acid membranes (PFSA, such as Nafion[®], Gore[®], Flemion[®], Fumion[®], Aquivion[®], or 3M[®] Membrane) seem appropriate in terms of conductivity from room temperature to 80 °C under 100 % relative humidity (RH) [14-16]. However, face to their expensive price and specific processing parameters, a broad range of fluoro-based polymers and nanocomposites have been developed to enlarge the membrane applications window [17, 18]. In that frame, three methods have been mainly reported: *i*) proton conductive groups have been incorporated within the (co)polymer backbone (by grafting or via synthesis) or from blending, *ii*) fillers have been introduced in a proton conductive (co)polymer, or *iii*) proton conductive fillers have been dispersed in non-proton conductive polymers to enhance the final properties. As an example, sulfonated moieties were for example grafted onto commercially available poly(vinylidene fluoride-*co*-HFP) copolymers (poly(VDF-*co*-HFP)) by using 4-hydroxybenzenesulfonic acid disodium salt.[19]. A range from 1.8 to 5.1 mol% grafted functions onto the poly(VDF-*co*-HFP) was obtained exhibiting ion exchange capacities from 0.27 to 0.61 meq.g⁻¹. Souzy et al. [20] synthesized

poly(VDF-*ter*-HFP-*ter*-MAF) terpolymers grafted by aryl sulfonic acids from the radical terpolymerization of α -trifluoromethacrylic acid (MAF) with VDF and HFP followed by the reduction of the carboxylic acid into hydroxyl ones and the further etherification reaction of these hydroxyl groups with 4-sulfonic acid phenol. From this approach, ionic exchange capacity, proton conductivity, and swelling rates reached 1.2 meq.mol⁻¹, 9 mS.cm⁻¹, and 58%, respectively. Hence, numerous nanoparticles have been incorporated into Nafion[®] membranes for PEMFC [21-23], such as SiO₂[24], TiO₂[25] or various cationic natural phyllosilicates [26] as well as needle-like clay, i.e. sepiolite [27,28]. Nevertheless, the final dispersion state of the nanofillers plays a key role on the proton conductivity of the resulting nanocomposite membranes. Recently, the fluorination of sepiolite was proved to be beneficial for its dispersion state in the Aquivion[®] membrane but slightly enhanced the proton conductivity compared to pristine sepiolite-based composite [28]. The proton conductivity can be brought out additionally through the modification of the filler surface. Ahmadian-Alama et al. [29] prepared a new PEMFC membrane by first modifying both the PVDF and the silica to create sulfonic acid groups and secondly produced composites with copolymer containing sulfonated segments (PMMA-*co*-PAMPS), i.e. a copolymer containing a miscible block with the grafted chains on the silica surface. They demonstrated that both water uptake and the IEC of the nanocomposite membranes were increased by increasing silica nanoparticles content. The maximum proton conductivity was 20 mS.cm⁻¹ at 25 °C for the nanocomposite membrane containing 10% silica nanoparticles. Niepceon et al. [30] prepared poly(VDF-*co*-HFP) based functional composites by grafting the silica with sulfonated polystyrene using atom transfer radical polymerization technique. Besides the incorporation of the preformed inorganic domains (functional or not), an alternative way was developed toward the sol-gel approach [31-33]. Based on very well-known hydrolysis-condensation reactions of alkoxysilane or metal alkoxides, that allows to lead to a better final filler dispersion in the polymer matrix due

to the fact that it proceeds from a reaction-induced phase separation process, fluoropolymer-based nanocomposites with SiO₂ or titanium dioxide were obtained via the *in situ* sol-gel of tetraethoxysilane and titanium isopropoxide, to enhance the mechanical properties and durability, respectively [34-41]. In that context, Sel *et al.* achieved hybrid fuel cell membranes from terpolymers based on VDF, vinyl tri(ethoxy)silane, and perfluoro(4-methyl-3,6-dioxaoct-7-ene sulfonyl fluoride (PFSFVE) further hydrolyzed and simultaneously condensed, leading to membranes with a conductivity of 12 mS.cm⁻¹ at 140 °C [42]. Xu *et al.* [43] filled Nafion[®] by a modified *in situ* sol-gel method and showed that the low humidity fuel cell performance at elevated temperatures was improved by almost 50%. Recently, Choi *et al.* [44] carried out similar approach to create titanium dioxide into Nafion[®] membrane. However, all these studies are dealing with solutions instead of proceeding in bulk due process limitations and formation of agglomerates of inorganic fillers in molten fluoropolymers. Face to this issue, a new alternative was developed by Bounor-Legaré *et al.* [45], combining reactive processing and sol-gel chemistry hence giving the opportunity to *in situ* create functionalized filler in a polymer molten matrix. This approach was already adopted to design fire-retardant polyamides and antibacterial polypropylene (PP). For example, diethylphosphatoethyltriethoxysilane (SiP) or 9,10-dihydro-9-oxa-10-phosphaphenanthrene (DOPO) based organophosphorous alkoxy silane were hydrolyzed and condensed during the polyamide extrusion step leading to the formation of 2wt% of phosphorus-containing silica [46,47]. For the bactericide properties, titanium tetrabutoxide was submitted to sol-gel reactions during the PP extrusion [48, 49].

Thus, this work is devoted to challenging reactive extrusion to produce membranes for PEMFC taking into account some sol-gel process of silicon alkoxides in a molten fluoropolymer. The objective of this study deals with the processing of new proton-conducting membranes by reactive extrusion of conventional non-functional fluoropolymers

with a functional trialkoxysilane (able to undergo oxidization modification to display sulfonic acid group) in the presence of a compatibilizing agent. Our previous work [50,51] demonstrated the possibility to prepare new fluoropolymers/functional silica based-nanocomposites for fuel cell membrane application by combining reactive extrusion and *in situ* formation of the inorganic phase by the sol-gel chemistry. Original membranes were synthesized by extrusion without any solvent. Significant contribution of the functional precursor (3-mercaptopropyltriethoxysilane, denoted 3-MPTES) was evidenced for reducing the size of inorganic-rich domains. However, this improvement did not allow obtaining significant protonic conductivities due to a low ionic exchange capacity due to the hindrance of oxidizable functions that are mainly trapped by the aggregation of the inorganic domains as well as inside the inorganic-rich domain. Therefore, it was of interest to tailor the morphology of the issued nanocomposites membranes. In that frame, polymeric interfacial agents were specifically synthesized. The common features of these ones lie on the hydrophobic character of the fluorinated main chain and the presence of a hydrophilic function able to interact with the poly(VDF-*co*-HFP) matrix and the inorganic phase, respectively. Thus, a better interfacial adhesion should be achieved in the new nanocomposites material resulting in a decrease of the surface tension, i.e. leading to lower diameter particles which display a higher surface area. Two families of interfacial agents were developed: *i*) fluorinated poly(VDF-*co*-M) copolymers with different concentrations of α -trifluoromethacrylic acid as comonomer. Besides, through its technology developed in the early 2000s, Arkema Co. offers *ii*) maleic anhydride (MA)-grafted poly(VDF-*co*-HFP) in different concentrations. The presence of MA group should also improve interfacial adhesion between the fluorinated matrix and the inorganic-rich phase.

2. Experimental

2.1 Materials and reagents

All reagents were used as received unless stated otherwise. Nafion NR112[®] from Sigma-Aldrich was used as a reference. 1,1-difluoroethylene (vinylidene fluoride, VDF), poly(VDF-*co*-HFP) copolymer (Kynar Flex 2750-10[®]), and maleic anhydride-grafted poly(VDF-*co*-HFP) [ADX[®], poly(VDF-*co*-HFP)-*g*-MA] copolymers were kindly offered by Arkema Co. (Pierre Benite, France). Kynar Flex 2750-10[®] ($M_n = 135,000 \text{ g}\cdot\text{mol}^{-1}$) is characterized by a 16% wt of HFP, a relatively low viscosity of about 900 Pa.s at 230 °C. Its melting temperature and crystallinity are 135 °C and 25-27%, respectively. The poly(VDF-*co*-HFP)-*g*-MA copolymer (**Figure 1**) was obtained by grafting maleic anhydride (MA) onto poly(VDF-*co*-HFP) by γ -rays irradiation. The grafted maleic anhydride content was ranging between 0.12 and 0.75 wt%. It has the advantage of maintaining properties close to those of the initial poly(VDF-*co*-HFP) Kynar[®] copolymer with a high decomposition temperature (>350 °C).

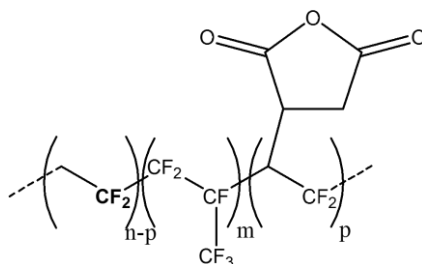


Figure 1 : Structure of the poly(VDF-*co*-HFP)-*g*-MA obtained by grafting maleic anhydride onto poly(VDF-*co*-HFP) copolymer

The inorganic precursors, i.e. a linear precondensed polydimethoxysiloxane (PDMOS, boiling point of 220°C, and repetitive molar mass of 106.2 g.mol⁻¹) and 3-mercaptopropyltriethoxysilane (MPTES, boiling point of 210°C, and a molar mass of 238.4 g.mol⁻¹) were purchased from ABCR and used as received.

α -trifluoromethacrylic acid (MAF) was a gift from Tosoh Finechemicals Co. (Shunan, Japan).

Tert-butylcyclohexyl peroxydicarbonate (Perkodox[®]16, purity 97%) and *tert*-butyl

peroxypivalate (TBPPi, purity 75%) were bought from AkzoNobel (Chalons-sur-Marne, France). Reagent Plus grade from dimethyl carbonate (DMC, purity >99%) and pentane were purchased from Sigma-Aldrich. Deuterated dimethyl sulfoxide (DMSO- d_6) and deuterated acetone (acetone- d_6), used for NMR spectroscopy, were supplied from Euroiso-top (Grenoble, France) (purity >99.8%). Ethanol and hydrochloric acid (10^{-2} N) for the prehydrolysis reactions were purchased from Aldrich and used as received. Distilled water and 50 wt% hydrogen peroxide were used for the chemical oxidization of mercapto groups into sulfonic acid function. NaCl and NaOH solutions used for ionic exchange capacity measurements were obtained from Acros.

2.2. Reactive extrusion

A DSM Micro 15 laboratory vertical micro-extruder (15 cm^3) with double intermeshing counter-rotating screws and a manual floodgate allowing either extrusion or recirculation was used to carry out the reactive extrusion at $200\text{ }^\circ\text{C}$ with a rotation speed of 100 rpm. A typical curve obtained during the extrusion process is depicted in **Figure 2**. The recorded normal force is a signature of viscosity changes in the reactive medium. The poly(VDF-*co*-HFP) was introduced at point (a). After polymer melting, the prehydrolyzed alkoxy silane solution was added by a syringe at the top of the extruder (b). Then, under shearing and temperature, the hydrolysis-condensation reactions took place and enabled to produce the inorganic network evidenced by the increase of the torque value (point c). Finally, the poly(VDF-*co*-HFP) based nanocomposite was extruded through a film die (d) and was further processed via a calendaring device. The film stretching allows reaching thicknesses under $200\text{ }\mu\text{m}$ for a final screw rotation speed of 60 rpm and a rolling speed of $50\text{ rad}\cdot\text{s}^{-1}$. Through the reaction extrusion based process, massive solid membranes are directly obtained without any use of

solvent. The by-products created during inorganic phase creation is methanol and ethanol which are evaporated during the process due to their low boiling points.

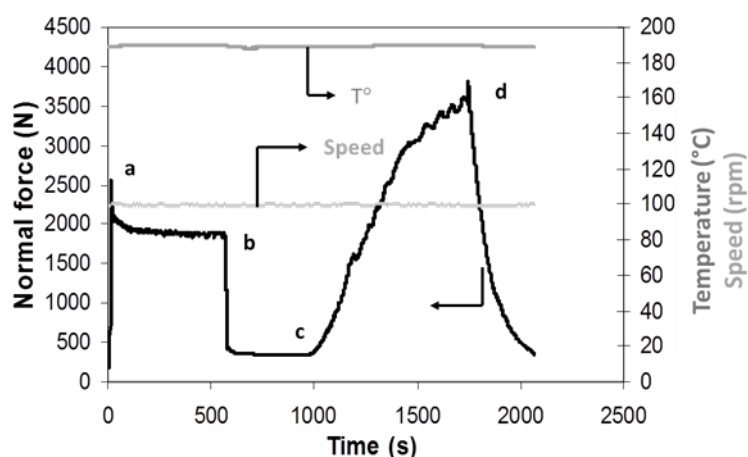


Figure 2: Extrusion process for the DSM micro-extruder: a, addition of poly(VDF-co-HFP); b, addition of inorganic precursor solution; c, starting of the formation of the inorganic phase; d, extrusion of the polymer composite. (—) Normal Force (N), (---) Speed (rpm) and (····) Temperature (°C)

2.3 Description of the various chemical routes

a) Synthesis of the poly(VDF-co-MAF) interfacial agent

The radical copolymerization of VDF with MAF (**Figure 3**) was performed in a 100 mL Hastelloy autoclave Parr system (HC 276) which is equipped with a manometer, a mechanical Hastelloy anchor, a rupture disk (3000 PSI), inlet and outlet valves, and a Parr electronic controller (for regulating the stirring speed and heating).

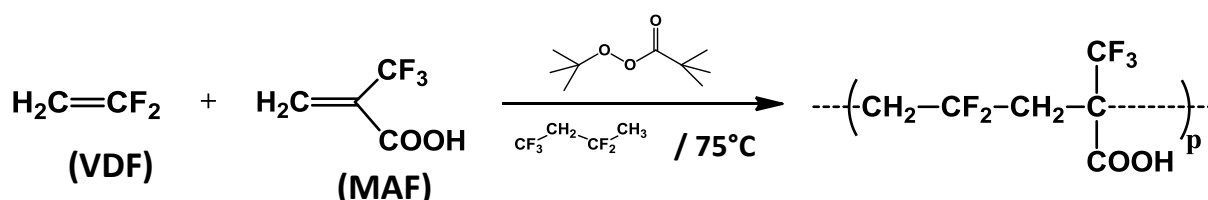


Figure 3: Radical copolymerization of VDF with α -trifluoromethacrylic acid (MAF) initiated by *tert*-butyl peroxyvalate (TBPPi)

A typical copolymerization of VDF with MAF was carried out as follows: initially, a solution composed of *tert*-butylcyclohexyl peroxydicarbonate (P-16, 2.276 g, 5.72 mmol) or *tert*-butyl peroxyvalate (TBPPi, 1.326 g, 5.72 mmol), MAF (13.7 g, 0.0978 mmol) in acetonitrile (30 mL) 1,1,1,3,3-pentafluorobutane (30 mL) was degassed by nitrogen bubbling for 30 min. During this time, the autoclave was checked for any leaks by pressurizing it with 30 bars of nitrogen. It was then put under vacuum ($40 \cdot 10^{-6}$ bar) for 30 min to remove residual traces of oxygen. The above solution was transferred into the autoclave under vacuum via a funnel tightly connected to the introduction valve of the autoclave. After this, the reactor was cooled in a liquid nitrogen bath, and VDF (27 g, 0.42 mol) was transferred through the autoclave inlet valve while monitoring its amount by double weighing (i.e., the difference of mass before and after filling the autoclave with VDF). The reactor was then allowed to warm up to ambient temperature and heated to the target reaction temperature (60 °C for P-16 or 74 °C for TBPPi) under mechanical stirring and the evolutions of pressure ($P_{\max} = 33$ bar) and temperature were recorded. The reaction was stopped after ca. 10-12 h when the autoclave pressure ceased to drop anymore, by placing the autoclave in an ice bath. The unreacted gaseous VDF monomer was purged off and the content of the autoclave was transferred into a round bottom flask. Then, the solvent and possible unreacted VDF dissolved in the total product mixture was completely removed under vacuum. The resulting crude product was then dissolved in acetone and precipitated from chilled pentane, filtered and finally dried under vacuum ($20 \cdot 10^{-3}$ bar, 50 °C) for 15 h. The polymer, as an off-white solid (29.7 g, 70% yield), was characterized by ^1H and ^{19}F NMR spectroscopies.

^1H NMR (400 MHz, DMSO- d_6 , δ ppm): 2.2 to 2.4 (m, $-\text{CF}_2\text{CH}_2-\text{CH}_2\text{CF}_2-$ reverse VDF-VDF T-T dyad addition and $-\text{CH}_2\text{C}(\text{CF}_3)\text{CO}_2\text{H}-$); 2.60 to 3.20 (m, $-\text{CH}_2\text{CF}_2-\text{CH}_2\text{CF}_2-$,

normal VDF–VDF H-T dyad addition), 6.3 (tiny tt, $^2J_{\text{HF}} = 55.0 \text{ Hz}$, $^3J_{\text{HH}} = 4.6 \text{ Hz}$) –CH₂CF₂–H end-group originated from the transfer of proton to solvent or polymer or from the back biting [52].

¹⁹F NMR (376 MHz, DMSO-*d*₆, δ ppm): –91.5 to –93.5 (–CH₂CF₂–CH₂CF₂–normal VDF–VDF H-T dyad addition); –94.7 (–CF₂ of VDF in the VDF–MAF dyad); –114 (–CH₂CF₂–CF₂CH₂–CH₂, reverse VDF–VDF H-H dyad addition); –114.5 (tiny dtt, $^2J_{\text{HF}} = 55.0 \text{ Hz}$, $^3J_{\text{HF}} = 16.0 \text{ Hz}$ and $^4J_{\text{FF}} = 6 \text{ Hz}$, CF₂–CH₂CF₂–H, chain-end from transfer); –116.2 (–CH₂CF₂–CF₂CH₂–CH₂, reverse VDF–VDF H-H dyad addition).

This procedure enabled us to prepare a wide range of poly(VDF-*co*-MAF) interfacial agents with MAF concentration ranging from 6 to 35 mol.%. In the text below, they will be denoted PVDF-*co*-MAF x where x corresponds to the MAF mole concentration in the copolymer.

b) Hydrolysis-condensation reactions

The inorganic phase was synthesized from sol-gel reactions of the inorganic precursors (**Figure 4**). First, the hydrolysis of the alkoxide group into a hydroxyl group occurred in the presence of water (**Figure 4 (1)**). Then, the hydroxyl group reacted with an alkoxide one to yield a siloxane bond and the corresponding alcohol or another hydroxyl to form a siloxane bond and water (**Figures 4 (2) and 4 (3)**). The hydrolysis reaction is favoured in acidic conditions whereas the condensation reaction is favoured in basic conditions.

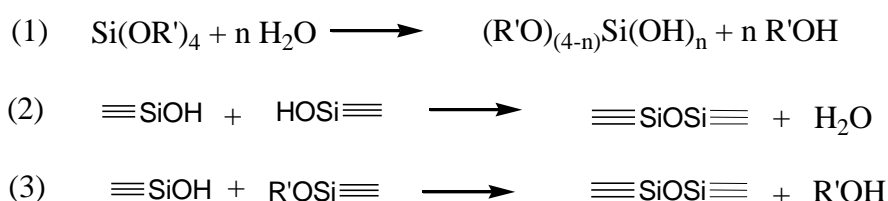


Figure 4 : Hydrolysis-condensation reactions of alkoxy silane inorganic precursors

Our first work [50], dedicated to a proof-of-concept to design PVDF/functionalized silica for PEMFC, evidenced that a pre-hydrolysis step was necessary for a proper *in situ* generation of the functionalized silica according to the reactive processing conditions. Hence, a water/alkoxy ratio (R_0) of 0.5 was required for a high sol-gel condensation reaction yield. The ratio of the functional alkoxy silane-to-structural inorganic precursor (R_1) defines the theoretical proton conductivity according to the -SH groups concentration which can be oxidized into sulfonic acid functions. It was also demonstrated that the functional inorganic precursor, i.e. 3-mercaptopropyltriethoxysilane (MPTES), being more soluble initially in the poly(VDF-*co*-HFP) matrix, compared to initially non-soluble polydimethylsiloxane allows a finer inorganic-rich phase dispersion with smaller size due to a compatibilizing effect. As a consequence, in this work, the experimental concentrations were adapted to reach 15 wt% of inorganic-rich phase with a theoretical ionic exchange capacity (IEC) of 2 meq.g⁻¹ and the inorganic precursors were pre-hydrolyzed at room temperature for 2 hours before being introduced into the molten polymer matrix.

c) Chemical modification of thiol into sulfonic acid function

In order to obtain proton conductivity, thiol groups were oxidized [53] with a 50 wt% hydrogen peroxide solution. The extruded films were immersed in H₂O₂ for 6 days at room temperature under stirring and then rinsed in deionized water for 24 h.

2.4 Characterization methods

Nuclear Magnetic Resonance (NMR) Spectroscopy.

The compositions and microstructures of the poly(VDF-*co*-MAF) copolymers were determined by ¹H and ¹⁹F NMR spectroscopies using a Bruker AC 400 Spectrometer (400 MHz for ¹H and 376 MHz for ¹⁹F) using DMSO-*d*₆ as solvent. Coupling constants and

chemical shifts were given in Hertz (Hz) and parts per million (ppm), respectively. The experimental conditions for recording ^1H [or ^{19}F] NMR spectra were as follows: flip angle 90° [or 30°], acquisition time 4.5 s [or 0.7 s], pulse delay 2 s [or 5 s], number of scans 32 [or 64], and a pulse width of 5 μs for ^{19}F NMR.

Fourier Transform Infrared (FTIR) Spectroscopy.

FTIR analyses of the copolymers were performed using a PerkinElmer Spectrum 1000 in ATR mode with an accuracy of $\pm 2\text{ cm}^{-1}$.

Scanning electron microscopy

Morphology was studied by scanning electron microscopy (SEM) on a Hitachi microscope S800 at an acceleration voltage of 15 kV. The samples were first prepared by cryo-ultramicrotomy at -65°C with a Leica EMFCS microtome device equipped with a diamond knife. This technique was used to prepare a specific planar surface. Samples were then sputter-coated under vacuum with carbon.

Elemental Analysis

Sulfur element was assessed by coulometry, by combustion in the oxygen of the sample in a furnace at $1,320^\circ\text{C}$ with formation of CO_2 and SO_2 . The SO_2 formed was then determined in a three-chamber electrolysis cell. The sulfur concentration allowed to calculate the theoretical ionic exchange capacity considering that all the $-\text{SH}$ groups were oxidized into $-\text{SO}_3\text{H}$.

Ionic exchange capacity

The ionic exchange capacity (IEC) was evaluated according to two different methods. The indirect dosing was carried out on the oxidized membrane immersed in 2 M NaCl solution for

24 h to exchange protons with sodium ions. Then, the resulting amount of acid chloride was estimated by titrimetry using a 5×10^{-3} M NaOH solution and phenolphthalein reagent. From this dosing, the IEC value (in meq.mol^{-1}) can be deduced considering the following equation (4).

$$IEC = \frac{C_{\text{NaOH}} \times V_{\text{NaOH}}}{m} \times 1000 \quad (4)$$

where m , C_{NaOH} , and V_{NaOH} are the sample mass, the concentration and added volume of NaOH solution, respectively.

On the other hand, the theoretical IEC values were also calculated from the elemental analysis of sulfur content.

Water uptake

Films were soaked in water for 24 hours and the dry (t_d) and wet (t_w) thicknesses were measured. Thus, the water uptake associated to the thickness variation change is given by the following equation:

$$\Delta t(\%) = \frac{(t_w - t_d) \times 100}{t_d} \quad (5)$$

Proton conductivity

The proton conductivity of the nanocomposite films was measured using an *ex situ* electrochemical impedance spectroscopy (EIS) technique and a laboratory-built cell composed of two parallel wire electrodes of platinum separated by 10 mm (through plane). To carry out the analysis, the sample ($5 \times 20 \text{ mm}^2$) was first immersed in deionized water for 24 h. The two probes were used to assess both source current and voltage drop and were in contact with the proton-activated samples in deionized water at room temperature. The impedance assessments were realized using a Novocontrol impedance analyzer with an SI

1255 spectrometer in the frequency range of 30 MHz to 10 Hz. Nyquist plotting of real (Z') and imaginary (Z'') parts of the components of impedance were determined and the conductivity, σ , was calculated from the impedance data using the formula:

$$\sigma (mS/cm) = \frac{L}{Rxlxt} \quad (6)$$

where L (in cm) is the distance between electrodes, R (in kOhm) the membrane resistance derived from the real axis intersect at high frequencies, and l (in cm) and t (cm) are the width and thickness of the sample, respectively. Finally, we estimate that the error is less than 10% of the measurement.

3. Results and discussion

Untreated nanofillers, such as hydrophilic silica, cannot be easily dispersed in fluoropolymers. Thus, various authors proposed to functionalized the surface of nanofillers via a “grafting from” polymerization of fluorinated monomers [54] leading to covalently bond a fluorinated polymer to the nanoparticles. Other routes [55, 56] were described including the one taking into account the polar interactions established at the nanoparticle surface (e.g. nickel) with poly(methacrylic acid)-*b*-PVDF-*b*-poly(methacrylic acid) triblock copolymers. Another strategy deals with the design of interfacial agents, i.e. compatibilizers, which can lead to the creation of specific, interactions between non-functional poly(VDF-*co*-HFP) copolymer and filler surface. According to this route, a poly(VDF-*co*- α -trifluoromethacrylic acid) copolymer (denoted poly(VDF-*co*-MAF) could be considered [57-67]. By adopting such an approach, to the use of a chemically modified poly(VDF-*co*-HFP) matrix could be envisaged [63-67]. Thus, poly(VDF-*co*-HFP) grafted maleic anhydride (poly(VDF-*co*-HFP)-*g*-MA, ADX[®]) copolymers are considered. The consequences of these different routes on the *in situ*

generated inorganic-rich dispersed phase, i.e. the final morphologies, and the resulting electrochemical properties, in particular the ionic conductivity, are studied.

3.1. Reactive extrusion of poly(VDF-*co*-HFP) /poly(VDF-*co*-MAF) /SiO₂ : Role of the poly(VDF-*co*-MAF) interfacial agent

The poly(VDF-*co*- α -trifluoromethacrylic acid) copolymer was considered as an interfacial agent in poly(VDF-*co*-HFP)/ SiO₂ materials as the carboxylic acid may develop specific interactions with the condensed inorganic species and the fluorinated matrix. As described previously [57], this interfacial agent was obtained by radical copolymerization of VDF with MAF since it is possible to tune the content of carboxylic acid in the resulting copolymers. This enables to reduce the interfacial tension between the inorganic-rich dispersed domains designed during the reactive extrusion step and the poly(VDF-*co*-HFP) copolymer. First, the description of the copolymers is supplied, followed by the formulation of the nanocomposites materials that further undergoes reactive extrusion (including the influence of MAF concentration) before being processed as films. Then, the oxidation of the mercaptan function into sulfonic acid is reported.

3.1.1) Radical copolymerization of VDF with MAF

This reaction can be initiated by various radical initiators. We have chosen *tert*-butylcyclohexyl peroxydicarbonate having a half-life time of one hour at 60 °C. Additionally, *tert*-butyl peroxyvalate (TBPPi) that also displays a half-life time of one hour at 74 °C was also used. Several initial [VDF]/[MAF] molar ratios were considered. As MAF does not homopolymerize [68], it is a suitable comonomer for VDF (the copolymerization yields were ranging from 65 to 88 %). After copolymerization and purification, the poly(VDF-*co*-MAF)

copolymer was characterized by NMR spectroscopy and MALDI-ToF. The ^{19}F NMR spectrum of the copolymer exhibits the expected signals centered at -69, -92, and -113 and -116 ppm assigned to the CF_3 group of MAF and of CF_2 of normal Head-to-Tail and reversed Head-to-Head addition. As expected from feed MAF content higher than 20 mol. %, a quasi-alternated structure is favored showing an intense signal centered at -94.7 ppm assigned to CF_2 in the $-\text{CH}_2\text{CF}_2-\text{CH}_2\text{C}(\text{CF}_3;\text{CO}_2\text{H})-$ dyad [57-64]. The ^1H NMR spectrum of the copolymer displays the expected signals characteristic of CH_2 in VDF (normal evidenced at 2.6-3.2 ppm, and reversed addition highlighted at 2.2- 2.4 ppm), those of CH_2 in MAF (ca. 2 ppm) and the singlet centered at 1.4 ppm attributed to *tert*-butyl end group coming from the initiator fragment. The MALDI-ToF spectrum of the alternated poly(VDF-*alt*-MAF) copolymer displays the same m/z unit of 204 assigned to $-\text{[CH}_2\text{CF}_2-\text{CH}_2\text{C}(\text{CF}_3;\text{CO}_2\text{H})]-$ dyad. This study focusses on the poly(VDF-co-MAF) copolymers containing 6, 13, 20, 28, and 35%mol of MAF.

3.1.2) Reactive extrusion

A solution of inorganic precursors leading to a theoretical IEC of 2 meq.g^{-1} in the resulting membrane was prepared for each nanocomposite material. In order to investigate the proof of concept, i.e. the design by an extrusion process of such membranes, two preliminary experiments (results not shown here and based on our previous [50, 51]) were conducted with either *i*) 8 wt% of poly(VDF-co-MAF) copolymer (denoted as PVDF-*co*-MAF 6) for a system with 15wt % of inorganic phase or with *ii*) 5 wt% of PVDF-*co*-MAF 6 and 20 wt% of generated equivalent SiO_2 . The interfacial agent was introduced for all the systems at step b (**Figure 1**) during the addition of the precursor solution in the molten poly(VDF-*co*-HFP) matrix. For both experiments, a high increase of the viscosity was observed up to the hindrance of the material extrusion. Due to the strong interaction between the reactive groups

brought up between the compatibilizing agent and inorganic domains, 5 wt% of interfacial agent and 15 wt% of equivalent SiO_2 phase were selected.

a). Influence of the MAF concentration on the nanocomposite morphologies of the resulting membranes

According to the description provided in **Figure 2**, it is observed in all of these cases, after injection of the inorganic precursor solution (at point b), a clear increase of the normal force related to the increase of viscosity and to the elastic character of the medium, i.e. to the *in situ* condensation of silanol species leading to inorganic-rich network as dispersed particles (**Figure 5**).

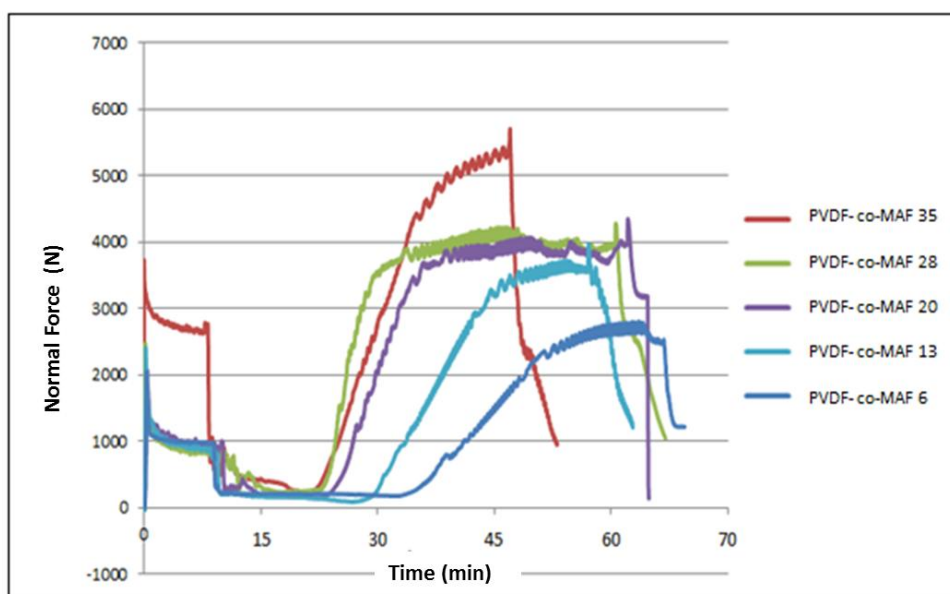


Figure 5: Normal force changes versus blending time for each reactive system based on poly(VDF-*co*-HFP), 5 wt% poly(VDF-*co*-MAF), and SiO_2 precursors (leading to the *in situ* generation of 15% wt equivalent SiO_2 and 2 meq of theoretical ionic exchange capacity) for various MAF content

It can be also clearly evidenced that the induction time preceding the inorganic-rich domain generation is dependent on the MAF content of the compatibilizing copolymer. In fact, this one decreases from 28 min with the addition of the PVDF-*co*-MAF 35 down to 13 min with the addition of the PVDF-*co*-MAF 6. This means that the increase of the trifluoromethacrylic acid content favors the interactions which can be established during the condensation reactions conducting to formation of the inorganic-rich particles, i.e. contributes to the decrease of the interfacial tension between fluorinated polymer matrix and inorganic-rich phase. As a consequence, the dispersed inorganic-rich phase exists as smaller particles leading to an increase in the normal force. The resulting morphologies studied by SEM, shown in **Figure 6** evidenced inorganic-rich domain sizes from 3 to 6 μm with good interfacial adhesion. These inorganic-rich domains were even smaller (less than 1 μm in diameter) in the cases of low MAF concentrations, i.e. 13 and 6 wt.% for PVDF-*co*-MAF 13 and PVDF-*co*-MAF 6, respectively.

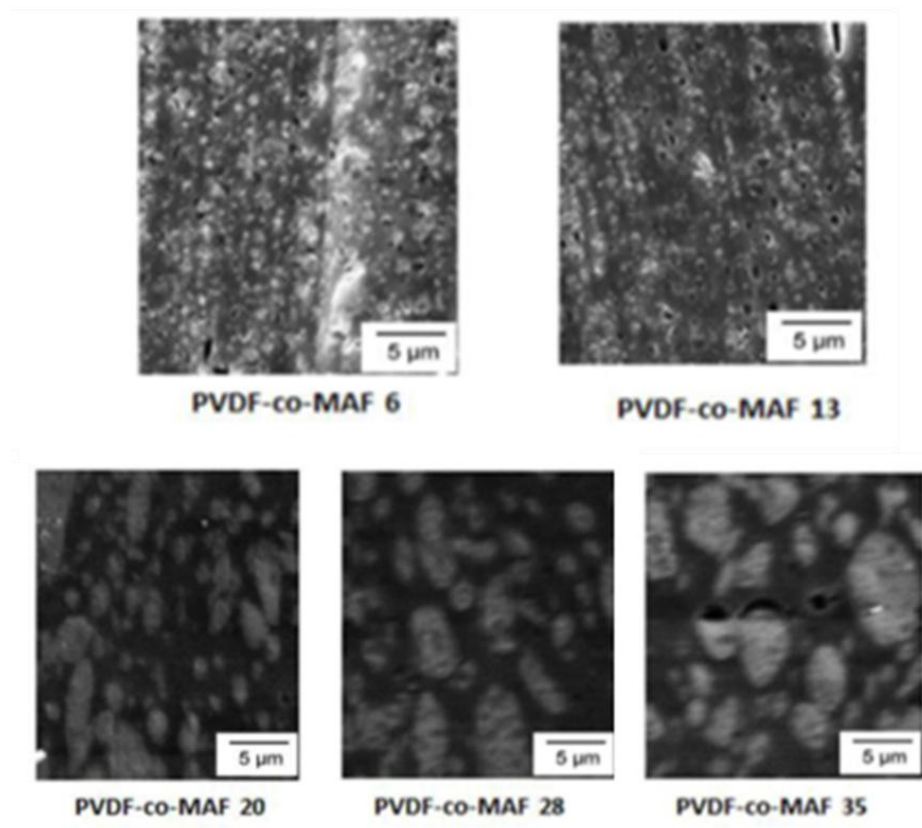


Figure 6: Scanning electron microscopy (SEM) micrographs of poly(VDF-*co*-HFP) /5wt. % poly(VDF-*co*-MAF)/15 wt% equivalent SiO₂ nanocomposites materials for various MAF concentration in poly(VDF-*co*-MAF) copolymer used as interfacial agent (from 6 to 35 mol%)

Overall, an increasingly fine dispersion was observed for low MAF content in poly(VDF-*co*-MAF) copolymer. This suggests the existence of a critical MAF concentration for which the interactions established between the organic and inorganic phases are favored. As MAF concentration is high, interactions between the acidic groups of the poly(VDF-*co*-MAF) are favored leading to a decrease of the interactions at the inorganic-rich phase/poly(VDF-*co*-HFP) interface. Due to this phenomenon, the silica phase could form aggregates having larger sizes. The changes of morphology can also be related to the induction time which is favorable to a better dispersion as it was also previously observed in the non-compatibilized poly(VDF-*co*-HFP) /SiO₂ composites [50,51]. Actually, a longer induction time is associated to a progressive formation of the inorganic-rich phase and improved interfacial interactions.

b) IEC conductivity and physical properties as a function of MAF content of poly(VDF-*co*-MAF) copolymers used as interfacial agents

The specific characteristics such as the water uptake of the resulting films were measured as well as the IEC conductivity by indirect dosing after oxidization of the mercaptan groups with hydrogen peroxide. IEC analyses by elemental analysis were also performed and compared to those measured by titration. Finally, the conductivity was determined and compared to that of the nanocomposite material produced without any compatibilization and to that of Nafion® in similar conditions. **Table 1** summarizes all the results obtained for each resulting films.

Table 1 : Physical and electrochemical properties of poly(VDF-co-HFP) /5wt. % poly(VDF-co-MAF)/SiO₂ (15wt. % of equivalent SiO₂) nanocomposites materials depending on the MAF concentration (comparison with the non- compatibilized).

Interfacial agent poly(VDF-co-MAF)	PVDF-co- MAF 6	PVDF-co- MAF 13	PVDF-co-MAF 20	PVDF-co- MAF 28	PVDF-co-MAF 35	PVDF-HFP/SiO ₂
Water uptake (%) a	14	13	13	14	13	11
IEC Titration (meq/g) ^b	1.32	1.10	0.90	1.10	0.98	0.80
IEC Elemental analysis (meq/g) ^c	1.50	1.20	1.00	1.10	1.04	
Conductivity (mS/cm) ^d	78	28	16	18	14	13

a) From equation (5)

b) IEC Titration from equation (4)

c) IEC from S elemental analysis

d) Conductivity from equation (6)

In all cases, the IECs determined by indirect titration, is strongly dependent on the presence of an interfacial agent. Furthermore, it can be noticed that these IEC values are higher for low MAF content. This phenomenon could be related to the morphology of this nanocomposite for which the size of the inorganic-rich domains is the lowest one (below 1 μm as diameter). In fact, as the accessibility of functional sites enhanced by a finer dispersion of the inorganic-rich domains, i.e. a larger surface deployed for interactions. Nevertheless, such fine morphologies cannot fulfill the objectives to get an IEC level up for 2 meq.g^{-1} to be reached and this trend observed through the titration assessment is also confirmed by the values determined by elemental analyses. However, it is observed for that the ionic concentration determined by elemental analysis give slightly higher results compared to indirect methods. In

fact, the elemental analysis technique considers all sulfur present whereas the titration could directly tailored from this parameter. The protonic conductivities measured for nanocomposites display obviously dependence of IEC with the morphology of the materials. The large conductivity improvement could be associated to the cooperative transport allowed by acidic groups. Thus, the nanocomposites could display higher protonic conductivities than that of Nafion[®] (for similar thickness of 74 μ m).

In addition, these results report similar results for water uptake of all the nanocomposites, and inorganic content. The water uptake content values (**Table 1**) are quite low compared to the Nafion considered as a reference.

3.2. Reactive extrusion of poly(VDF-co-HFP)-g-MA/SiO₂: Role of the maleic anhydride content

Besides the synthesis and introduction of an interfacial agent, i.e. poly(VDF-co-MAF), another approach is proposed in this study. The first step consists in bringing great ideas program, fluorinated polymer and the functional silica is to chemically modify the main matrix. In that frame, poly(VDF-co-HFP) grafted maleic anhydride [poly(VDF-co-HFP)-g-MA, ADX[®]] copolymers with maleic anhydride (MA) concentration ranging between 0.12 and 0.75 wt% were prepared and tested.

3.2.1) Influence of the MA concentration on the in situ generated morphologies of the nanocomposites

The same protocol as above was used. A solution of precursors corresponding to 15wt% of the expected created inorganic phase was prepared for each nanocomposite. As the MA concentration remains lower than 1 wt%, poly(VDF-co-HFP)-g-MA was considered as the matrix.

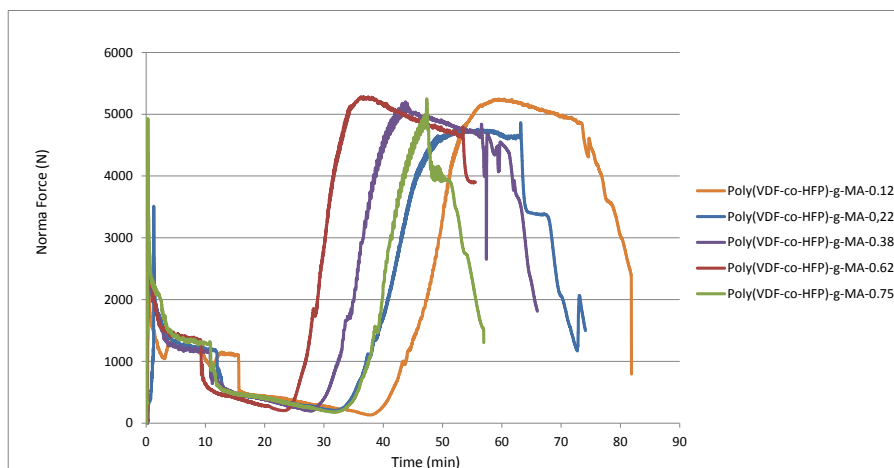


Figure 7: Normal force changes during processing time for various reactive systems leading to the *in situ* generation of 15% wt equivalent SiO_2 (2 meq of theoretical ionic exchange was targeted) poly(VDF-co-HFP)-g-MA (grafting ratio from 0.12 to 0.75 wt% of MA).

These nanocomposites synthesized with pre-hydrolyzed inorganic phase precursor solutions considered at room temperature for 2 hours, were characterized. The influence of the MA concentration in the poly(VDF-co-HFP)-g-MA copolymer on the induction time is clearly evidenced (**Figure 7**) except for the systems based on the PVDF-g-MA-0.75. The induction time decreases with the MA content in the poly(VDF-co-HFP)-g-MA. According to our studies, the higher is the MA content in poly(VDF-co-HFP)-g-MA considered as interfacial agent, led to favor the interactions with the growing inorganic-rich phase.

By comparing the morphologies (**Figure 8**) of poly(VDF-co-HFP)-g-MA-based nanocomposites materials, it shows that a distinct dispersion with the increase of the MA amount contained in the polymer matrix. Indeed, for the material based on poly(VDF-co-HFP)-g-MA-0.12 (0.12 wt% AM), poorly adhered inorganic-rich dispersed domains were observed. A better cohesion was highlighted for material synthesized with the poly(VDF-co-HFP)-g-MA-0.22 where inorganic-rich domains are increasingly embedded in the matrix. For 0.38 wt% of MA, the interfacial adhesion looks better but domains of size close to the micron

were formed. It is only for 0.62 wt% MA content that a good dispersion of the inorganic phase was observed with SiO₂-like domains of about 500 nm-size. These inorganic-rich domains, well distributed in the matrix, were even smaller in the case of higher MA ratio (0.75 wt%), i.e. for the poly(VDF-co-HFP)-g-MA-0.75 hybrid material, as shown in **Figure 9**.

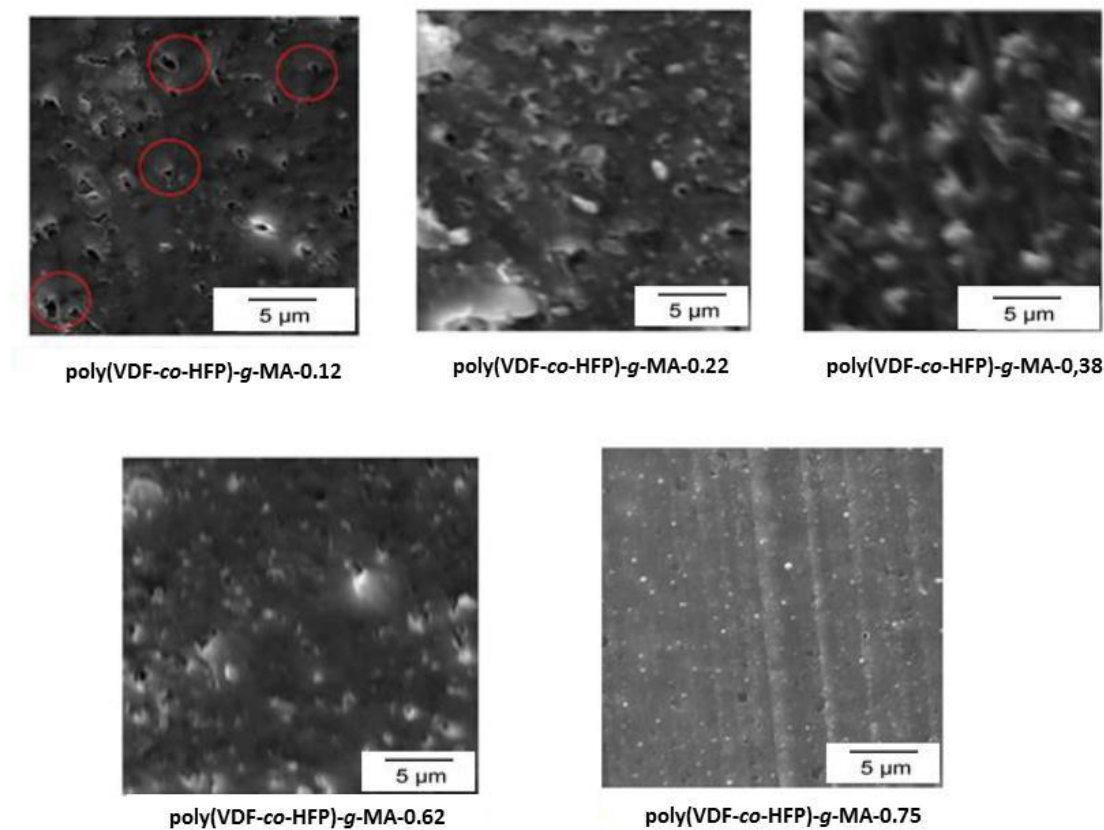


Figure 8: SEM images for poly(VDF-co-HFP)-g-MA/15 wt% equivalent SiO₂ composites depending of the concentration of MA grafted concentration (from 0.12 to 0.75 mol%). The red circles on the images for the poly(VDF-co-HFP)-g-MA-0.12 indicate the poor adhesion between the organic and inorganic phases.

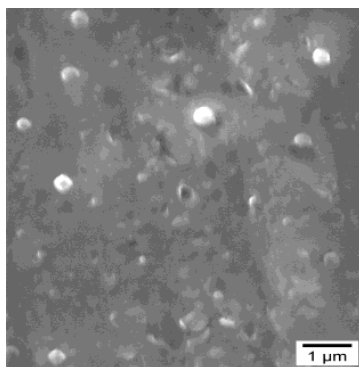


Figure 9 : SEM micrograph of the poly(VDF-co-HFP)-g-MA-0.75 (0.75wt% AM) nanocomposites at 2 meq and 15% equivalent SiO_2 at higher magnification

These inorganic-rich domains, which are only a few hundred nm-long, were obviously the result of the compatibilizing effect of MA. In fact, the corresponding groups could interact at the interface of the inorganic-rich domains in the structuring phase playing the role of an interfacial agent, thus preventing their aggregation.

3.2.2) IEC, conductivity, and others physical properties of the nanocomposites depending of the MA concentration

As in the previous cases, the ion exchange capacities (IEC) were determined by indirect titration and elemental analysis while the protonic conductivities were measured at room temperature under 100% humidity. The evolution of the water uptake is also reported in **Table 2**.

Table 2 : Physical properties of poly(VDF-co-HFP)-g-MA/ SiO₂ nanocomposites depending of the MA concentration

Nanocomposite	poly(VDF-co-HFP)-g-MA-0.12	poly(VDF-co-HFP)-g-MA-0.22	poly(VDF-co-HFP)-g-MA-0.38	poly(VDF-co-HFP)-g-MA-0.62	poly(VDF-co-HFP)-g-MA-0.75
Water uptake (%) ^a	12.5	12.8	13.4	13.7	13.8
IEC non-direct dosing (meq/g) ^b	0.80	0.90	1.02	1.10	1.20
IEC Elemental analysis (meq/g) ^c	0.90	1.00	1.01	1.12	1.25
Conductivity (mS/cm) ^d	8	20	27	35	54

a) From equation (5)

b) IEC Titration from equation (4)

c) IEC from S content measured by elemental analysis

d) Conductivity from equation (6)

First, the water uptake remains unchanged (12.5 to 13.8%) and comparable to the values previously obtained for the same inorganic content with the poly(VDF-co-MAF) and without any interfacial agent. Thus, it can be concluded that the water uptake depends primarily on the concentration of the hydrophilic phase contained in the materials (the value is 30wt% for the Nafion reference characterized in the same conditions). The IECs, determined by titration assessment, showed higher values (ranging from 0.8 to 1.2 meq.g⁻¹) than those of systems obtained with poly(VDF-co-HFP) only (0.8 meq.g⁻¹). This IEC increases as the morphology of the films becomes thinner and reaches a maximum of 1.2 meq.g⁻¹ in the case of the finer dispersion, i.e. for poly(VDF-co-HFP)-g-MA-0.75. Thus, this observation confirms the

influence of the morphology and therefore of the quality of the dispersion of inorganic-rich domains with the fluorinated polymer matrix over the IEC.

Nevertheless, it can be noted that these IECs remain lower than the expected 2 meq.g^{-1} value. This tendency is also confirmed by elemental analysis which reveals IECs of 0.9 and 1.25 meq.g^{-1} for poly(VDF-*co*-HFP)-*g*-MA-0.12 (0.12wt% MA) and poly(VDF-*co*-HFP)-*g*-MA-0.75 -based materials, respectively. As in the previous case, these latter values slightly higher than the ones determined via the dosing method confirm the effect of the sulfonic acid group reachability through the thinner morphology.

The change of the proton conductivity follows that of the ionic concentration. Therefore, it is observed that, thanks to the compatibility provided by MA in a sufficient amount, in the case of poly(VDF-*co*-HFP)-*g*-MA-0.75-based membrane, a protonic conductivity of 54 mS.cm^{-1} is obtained which is comparable to 52 mS.cm^{-1} reached for Nafion[®] NR112 in the same temperature and hydration conditions.

Overall, these results show the significant contribution of maleic anhydride functions for the dispersion state of the inorganic-rich phase. As a consequence, the accessibility of the functional sulfonic sites is dramatically enhanced leading to a higher ionic concentration and an increase of the proton conductivity.

3.3 Comparison between both systems

By comparing the morphologies of the different nanocomposites obtained from poly(VDF-*co*-MAF) as interfacial agent with those based on poly(VDF-*co*-HFP)-*g*-MA, it can be observed that the finer dispersions are obtained with the poly(VDF-*co*-HFP)-*g*-MA-0.75 (inorganic-rich domains have a mean diameter lower than 300 nm) or from the use of 5 wt% of PVDF-*co*-MAF 6 copolymer (inorganic-rich domains have a mean diameter from 500 nm to 1 μm),

respectively. However, the low molar mass of poly(VDF-*co*-MAF) copolymers (about 12,000 g.mol⁻¹ equivalent PMMA) are more favorable for displaying a large poly(VDF-*co*-HFP)/inorganic-rich phase interfacial surface leading to the highest IEC and conductivity. Other parameters can also be discussed to explain the difference observed between these two types of interfacial agents. The solubility parameters calculated from Fedors' method [69] are 15.18 and 15.89 (MPa)^{1/2} for the poly(VDF-*co*-HFP)-*g*-MA 0.75 and poly(VDF-*co*-MAF) 6, respectively. These values are close to each other and close to the value of 15.2 (MPa)^{1/2} calculated for the poly(VDF-*co*-HFP) matrix. Thus, it cannot explain the difference between both systems and pointed out the role of the chemical nature of the polar function on the adhesion between the inorganic and the organic phases. Besides, the viscosity (illustrated by the normal force evolution change) is very high for the nanocomposites processed with using the maleic anhydride-based derivatives. This phenomenon could be explained by the composition of the inorganic-rich phase which has a high concentration of sulfur remaining trapped, hence lowering the IEC and the protonic conductivities of the resulting membranes. As a consequence, despite a rather fine dispersion, the highest conductivity of these nanocomposites materials was 54 mS.cm⁻¹ while the ones based on poly(VDF-*co*-MAF) reached conductivities up to 78 mS.cm⁻¹.

4. Conclusion

Proton exchange membranes could be processed by reactive extrusion in one step *in situ*-functionalized SiO₂-like dispersed phase in a fluorinated matrix. To enhance the ionic conductivity by tailoring the interface between the matrix and the inorganic-rich phase, two approaches have been developed: *i*) the synthesis of poly(VDF-*co*-MAF) copolymers by conventional radical copolymerization of VDF with in different contents of MAF and *ii*) to

substitute the poly(VDF-co-HFP) matrix by its homologous grafted with maleic anhydride [poly(VDF-co-HFP)-g-MA]. The influence of the addition of such interfacial agents depending on the concentration of functional groups on the final morphology and electrochemical properties of membranes was studied (keeping a concentration of 15wt% of eq. silica and a theoretical IEC of 2 meq.g⁻¹). In particular, the oxidative hydrolysis of mercapto groups into sulfonic acid function enabled us to supply proton-conductive membranes. Their water uptakes (limited up to 15 wt%), IECs (experimental IEC ranged between 1.0 and 1.3 meq.g⁻¹) and conductivities up to 78 mS.cm⁻¹ (at room temperature and 100% RH) when 5 wt% of poly(VDF-co-MAF) was involved in the reactive processing were observed. This value reached also 54 mS.cm⁻¹ with the used of the poly(VDF-co-HFP)-g-MA-0.75 which is comparable to that of Nafion[®] NR112 (52 mS.cm⁻¹). These results pointed out the essential role of the interface and its influence on the accessibility to the sulfonic acid functions. This study paves the way to processing of original membranes in extruder without any solvent and can be regarded as a clean process that avoids any solvent usually required to cast membranes [70,71].

Acknowledgements

The authors thank the French National Agency (ANR, project PREMHYS, grant ANR- 09-MAPR-0004-01) for financial support, Arkema (Pierre Bénite, France), and Tosoh Finechemicals Corp. (Shunan, Japan) companies for supplying VDF and Kynar[®], and 2-trifluoromethacrylic acid (MAF), respectively.

References

- 1 Acar, C. A. Comprehensive evaluation of energy storage options for better sustainability. *International Journal of Energy Research*, **2018**, 42(12), 3732-3746.
- 2 Nakata, T.; Silva, D.; Rodionov, M. Application of energy system models for designing a low-carbon society. *Progress in Energy and Combustion Science*, **2011**, 37(4), 462-502.
- 3 Dominkovic, D.F.; Bacekovic, I.; Pedersen, A. S.; Krajacic, G. The future of transportation in sustainable energy systems: Opportunities and barriers in a clean energy transition, *Renewable and Sustainable Energy Reviews*, **2018**, 82 (Part 2), 1823-1838.
- 4 Newman, J.; Bonino, C.A.; Trainham, J.A. The energy future, *Annual Review of Chemical and Biomolecular Engineering*, **2018**, 9, 153-174.
- 5 Wang, Y.; Chen, K. S.; Mishler, J.; Cho, S. C.; Adroher, X. C. A review of polymer electrolyte membrane fuel cells: Technology, applications, and needs on fundamental research. *Applied Energy*, **2011**, 88, 981–1007.
- 6 Rath, R.; Kumar, P.; Mohanty, S. ; Nayak, S.K. Recent advances, unsolved deficiencies, and future perspectives of hydrogen fuel cells in transportation and portable sectors. *International Journal of Energy Research*. **2019**, 1-25.
- 7 Bruce, P. G.; Freunberger, S. A.; Hardwick, L. J.; Tarascon J-M., Li-O₂ and Li-S batteries with High Energy Storage. *Nature Materials*, **2012**, 11, 19-29.
- 8 Bouchet, R. ; Maria, S. ; Meziane, R. ; Aboulaich, A.; Lienafa L, Bonnet, J.P.; Phan, T.N.; Bertin, D.; Gignes, D.; Devaux, D.; Denoyel, R.; Armand M. Single-ion BAB triblock copolymers as highly efficient electrolytes for lithium-metal batteries *Nature Materials*, **2013**, 12, 452–457.

- 9 Costa, P.; Nunes-Pereira, J.; Pereira, N.; Castro, N.; Goncalves, S.; Lanceros-Mendez, S. Recent progress on piezoelectric, pyroelectric, and magnetoelectric polymer-based energy-harvesting devices. *Energy Technology*, **2019**, 7(7), 1-19.
- 10 Ameduri, B.; Boutevin, B. Well-architected fluoropolymers: Synthesis, properties, and applications, Elsevier, Amsterdam, **2004**.
- 11 Ameduri, B. From vinylidene fluoride (VDF) to the applications of VDF-containing polymers and copolymers - Recent developments and future trends. *Chemical Reviews* **2009**, 109, 6632-6686.
- 12 Yoshitake, M.; Watakabe, A. Perfluorinated ionic polymers for PEFCs (including supported PFSA) in: G.G Scherer (Ed.), *Fuel Cells I*, Springer Berlin Heidelberg, Berlin, Heidelberg, **2008**, 127-155.
- 13 Smith, D.W.; Lacono, S.T.; Lyers, S.S. Handbook of Fluoropolymers, Science, and Technology, Wiley, New York **2014**.
- 14 Hickner, M. A.; Ghassemi, H.; Kim, Y. S.; Einsla, B. R.; McGrath; J. E. Alternative polymer systems for proton exchange membranes (PEMs). *Chemical Reviews* **2004**, 104, 4587–4612.
- 15 Smitha, B.; Sridhar, S.; Khan, A.A. Solid polymer electrolyte membranes for fuel cell applications-A review, *Journal of Membrane Science* **2005**, 259, 10-26.
- 16 Drioli, E.; Giorno, L.; Fontananova, E. Comprehensive membrane science and engineering; Membrane Science and Technology; **2017**, Volume 1 ISBN: 9780444637758. Elsevier, Amsterdam.
- 17 Subianto, S.; Pica, M.; Casciola, M.; Cojocar, P.; Merlo, L.; Hards, G.; Jones D.J. Physical and chemical modification routes leading to improved mechanical properties of

- perfluorosulfonic acid membranes for PEM fuel cells, *Journal of Power Sources*, **2013**, *233*, 216-230.
- 18 Inamuddin, M. A.; Asiri, A. M. Organic-inorganic composite polymer electrolyte membranes, Springer International Publishing, Cham, Switzerland **2017**.
- 19 Taguet, A.; Ameduri, B.; Boutevin, B. Grafting of 4-hydroxybenzenesulfonic acid onto commercially available poly(VDF-co-HFP) copolymers for the preparation of membranes. *Fuel Cells* **2006**, *6(5)*, 331-339.
- 20 Souzy, R.; Boutevin, B.; Ameduri, B. Synthesis and characterizations of novel proton-conducting fluoropolymer electrolyte membranes based on poly(vinylidene fluoride-ter-hexafluoropropylene-ter- α -trifluoromethacrylic acid) terpolymers grafted by aryl sulfonic acids, *Macromolecules*, **2012**, *45*, 3145–3160.
- 21 Laberty-Robert, C.; Vallé, K.; Pereira, F.; Sanchez, C.; Design and properties of functional hybrid organic–inorganic membranes for fuel cells. *Chemical Society Review*, **2011**, *40*, 961-1005.
- 22 Kim, D. J.; Sang M.J.J. ; Nam S.Y. A review of polymer–nanocomposite electrolyte membranes for fuel cell application. *Journal of Industrial and Engineering Chemistry*. **2015**, *21*, 36-52.
- 23 Cele, N.; Ray, S.S. Recent progress on Nafion-based nanocomposite membranes for fuel cell applications. *Macromolecular Materials and Engineering*, **2009**, *294 (11)*, 12 719-738.
- 24 Ying, Y.P.; Kamarudina, S.K.; Masdar, M.S.; Silica-related membranes in fuel cell applications: An overview. *International Journal of Hydrogen Energy*, **2018**, *43(33)* 16068-16084.

- 25 Saccà, A.; Carbone, A.; Gatto, I.; Pedicini, R.; Freni, A.; Patti, A.; Passalacqua, E. Composites Nafion-titania membranes for Polymer Electrolyte Fuel Cell (PEFC) applications at low relative humidity levels: Chemical physical properties and electrochemical performance. *Polymer Testing*, **2016**, *56*, 10-18.
- 26 Alonso, R.H.; Estevez, L.; Lian, H.; Kellarakis, A.; Giannelis, E.P. Nafion-clay nanocomposite membranes: Morphology and properties. *Polymer*, **2009**, *50(11)*, 2402-2410.
- 27 Beauger, C.; Lainé, G.; Burr, A.; Taguet, A.; Otazaghine, B.; Rigaccia, A.; Nafion-sepiolite composite membranes for improved proton exchange membrane fuel cell. *Journal of Membrane Science*, **2013**, *430*, 167-179.
- 28 Woo, S.H.; Taguet, A.; Otazaghine, B.; Mosdale, A.; Rigacci, A.; Beauger, C.; Physicochemical properties of Aquivion/fluorine grafted sepiolite electrolyte membranes for use in PEMFC, *Electrochimica Acta*, **2019**, *319*, 933-946.
- 29 Ahmadian-Alama, L.; Kheirmand, M.; Mahdavia, H. Preparation, characterization and properties of PVDF-g-PAMPS/PMMA-co-PAMPS/silica nanoparticle as a new proton exchange nanocomposite membrane, *Chemical Engineering Journal*, **2016**, *284*, 1035-1048.
- 30 Niepceron, F.; Lafitte, B.; Galiano, H.; Bigarré, B.; Nicol, E.; Tassin, J.-F. Composite fuel cell membranes based on an inert polymer matrix and proton-conducting hybrid silica particles. *Journal of Membrane Science*, **2009**, *338*, 100-110.
- 31 Livage, J. Basic principles of sol-gel chemistry. In *Sol-Gel Technologies for Glass Producers and Users*; Aegerter, M. A., Mennig, M., Eds.; Springer US: Boston, MA, **2004**, 3-14.
- 32 Livage J, Henry M, Sanchez C., Sol-gel chemistry of transition-metal oxides, *Progress in Solid State Chemistry*, **1988**; *18*: 259-341.

- 33 Sanchez, C.; Livage, J. Sol-gel chemistry from metal alkoxide precursors. *New Journal of Chemistry*, **1990**, *14* (6–7), 513–521.
- 34 Valle, K.; Belleville, P.; Pereira, F.; Sanchez, C. Hierarchically structured transparent hybrid membranes by in situ growth of mesostructured organosilica in host polymer, *Nature Materials*, **2006**, *5*, 107-111.
- 35 Pereira, F.; Chan, A.; Valle, K.; Palmas, P.; Bigarre, J.; Belleville, P.; Sanchez, C. Design of interpenetrated networks of mesostructured hybrid silica and nonconductive poly(vinylidene fluoride)-co-hexafluoropropylene (PVdF-HFP) polymer for proton exchange membrane fuel cell applications, *Chemistry, an Asian Journal*, **2011**, *6*, 1217-1224.
- 36 Chanthad, C.; Xu, K.; Huang, H.; Wang, Q. Proton-conductive polymer nanocomposite membranes prepared from telechelic fluorinated polymers containing perfluorosulfonic acid side chains. *Journal of Polymer Science: Part A: Polymer Chemistry*, **2010**, *48*, 4800–4810.
- 37 Xu, K.; Chanthad, C.; Hickner, M.A.; Wang, Q.; Highly selective proton conductive networks based on chain-end functionalized polymers with perfluorosulfonate side groups; *Journal of Materials Chemistry*, **2010**, *20*, 6291–6298.
- 38 Alvarez, A.; Guzman, C.; Carbone, A.; Sacca, A.; Gatto, I.; Passalacqua, E.; Nava, R.; Ornelas, R.; Ledesma-Garcia, J.; Arriaga, L. G. Influence of silica morphology in composite Nafion membranes properties. *International Journal of Hydrogen Energy*, **2011**, *36*(22), 14725-14733.

- 39 Patil, Y.; Kulkarni, S.; Mauritz, K.A.; In Situ Grown Titania Composition for Optimal Performance and Durability of Nafion (R) Fuel Cell Membranes. *Journal of Applied Polymer Science*, **2011**, *121*(4), 2344-2353.
- 40 Jian-Hua, T.; Peng-Fei, G.; Zhi-Yuan, Z.; Wen-Hui, L ; Zhony-Qiang, S.; Preparation and performance evaluation of a Nafion-TiO₂ composite membrane for PEMFCs, *International Journal of Hydrogen Energy*, **2008**, *33*(20), 5686-5690.
- 41 Chung, M.; Zhang, Z.; Chalkova, E.; Wang, C.; Fedkin, M.; Komarneni, S.; Sharma, S.; Lvov, S., Proton conductive composite materials using functionalized and crosslinkable VDF/CFTE fluoropolymers and proton conductive inorganics.; *Electrochemical Society. Transactions*, **2007**, *11*, 35 (Proceedings of the 212th Meeting of the Electrochemical Society, Washington (USA), Oct. 7-12, 2007).
- 42 Sel, O.; Soules, A.; Ameduri, B.; Boutevin, B.; Laberty-Robert, C.; Gebel, G.; Sanchez, C. Original fuel-cell membranes from crosslinked terpolymers via a “sol-gel” strategy. *Advanced Functional Materials*, **2010**, *20*, 1090-1098
- 43 Xu, G.X.; Li, S.; Li, J.; Liu, Z.; Li, Y.; Xiong, J.; Cai, W.W.; Qu, K.G.; Cheng, H.S. Targeted filling of silica in Nafion by a modified in situ sol-gel method for enhanced fuel cell performance at elevated temperatures and low humidity. *Chemical Communications*, **2019**, *55*(38), 5499-5502.
- 44 Choi, B.; Ko, Y.; Kim, W. Low-humidifying Nafion/TiO₂ composite membrane prepared via in-situ sol-gel process for proton exchange membrane fuel cell. *Applied Chemistry for Engineering*, **2019**, *30*(1), 74-80.

- 45 Bounor-Legaré, V.; Cassagnau, P. *In situ* Synthesis of organic-inorganic hybrids or nanocomposites from sol-gel chemistry in molten polymers, *Progress in Polymer Science*, **2014**, *39*(8), 1473-1497.
- 46 Sahyoun, J.; Bounor-Legaré, V.; Ferry, L.; Sonnier, R.; Da Cruz-Boisson, F.; Mélis, F.; Bonhomme, A.; Cassagnau, P. Synthesis of a new organophosphorous alkoxysilane precursor and its effect on the thermal and fire behavior of a PA66/PA6 copolymer, *European Polymer Journal*, **2015**, *66*, 352-366.
- 47 Theil-Van Nieuwenhuysse, P.; Bounor-Legaré, V.; Bardollet, P.; Cassagnau, P.; Michel, A.; David, L.; Babonneau, F.; Camino, G. Phosphorylated silica/polyamide 6 nanocomposites synthesis by in situ sol-gel method in molten conditions: Impact on the fire-retardancy, *Polymer Degradation and Stability*, **2013**, *98*, 2635-2644.
- 48 Bahloul, W.; Bounor-Legaré, V.; David, L.; Cassagnau, P. Morphology and viscoelasticity of PP/TiO₂ nanocomposites prepared by in situ sol-gel method, *Journal of Polymer Science. Part B: Polymer Physics*, **2010**, *48*, 1213-1222.
- 49 Balhoul W., Melis F., Bounor-Legaré V., Cassagnau P., Structural characterisation and antibacterial activity of PP/TiO₂ nanocomposites prepared by an in situ sol-gel method *Materials Chemistry and Physics*, **2012**, *134*(1); 399-406.
- 50 Seck, S.; Magana, S.; Prébé, A.; Niepceron, F.; Bounor-Legaré, V.; Bigarré, J.; Buvat, P.; Gérard, J.F. PVDF-HFP/silica-SH nanocomposite synthesis for PEMFC membranes through simultaneous one-step sol-gel reaction and reactive extrusion. *Materials Chemistry and Physics*, **2015**, *163*, 54-62.
- 51 Gérard, J.F.; Niepceron, F.; Bounor-Legaré V.; Bigarré, J.; Galiano, H.; Mazabraud, P.; Buvat, P.; EP 2582451 (Avec CEA) : Procédé d'élaboration d'un matériau composite

comprenant une matrice polymérique et une charge consistant en des particules inorganiques échangeuses d'ions. 24 Avril **2013**.

- 52 Pianca, M.; Barchiesi, E.; Esposto, G.; Radice, S. End groups in fluoropolymers, *Journal of Fluorine Chemistry*, **1999**, *95* (1–2), 71-84.
- 53 Slade, R.C.T.; Varcoe, J.R. Proton conductivity in siloxane and Ormosil ionomers prepared using mild sulfonation methodologies, *Solid State Ionics*, **2001**, *145*, 127-133.
- 54 Prateek, Thakur, V.K.; Gupta, R.K.; Recent Progress on ferroelectric polymer-based nanocomposites for high energy density capacitors: Synthesis, dielectric properties, and future aspects. *Chemical Review*, **2016**, *116*(7), 4260-4317.
- 55 Voet, V. S. D.; Hermida-Merino, D.; ten Brinke, G.; Loos, K. Block copolymer route towards poly(vinylidene fluoride)/poly(methacrylic acid)/nickel nanocomposites. *RSC Advances*, **2013**, *3*, 7938-7946.
- 56 Voet, V. S. D.; Tichelaar, M.; Tanase, S.; Mittelmeijer-Hazeleger, M.C.; ten Brinke, G.; Loos, K. Poly(vinylidene fluoride)/nickel nanocomposites from semicrystalline block copolymer precursors. *Nanoscale*, **2013**, *5*, 184-192.
- 57 Souzy, R.; Ameduri, B.; Boutevin, B. Radical copolymerization of α -trifluoromethylacrylic acid with vinylidene fluoride and vinylidene fluoride/hexafluoropropene. *Macromolecular Chemistry and Physics*, **2004**, *205*, 476-485.
- 58 Boyer, C.; Ameduri, B. Iodine transfer copolymerization of vinylidene fluoride and α -trifluoromethacrylic acid in emulsion process without any surfactants, *Journal of Polymer Science Part A: Polymer Chemistry* **2009**, *47*, 4710-4722.

- 59 Patil, Y.; Ono, T.; Ameduri, B. Innovative trifluoromethyl radical from persistent radical as efficient initiator for the radical copolymerization of vinylidene fluoride with tert-butyl α -trifluoromethacrylate, *ACS Macro Letters* **2012**, *1*, 315-320.
- 60 Patil, Y.; Ameduri, B. Advances in the (co)polymerization of alkyl 2-trifluoromethacrylates and 2-(trifluoromethyl)acrylic acid, *Progress in Polymer Science*, **2013**, *38*, 703-709.
- 61 Patil, Y.; Alaaeddine, A.; Ono, T.; Ameduri, B. Novel method to assess the molecular weights of fluoropolymers by radical copolymerization of vinylidene fluoride with various fluorinated comonomers initiated by a persistent radical. *Macromolecules* **2013**, *46*, 3092-3106.
- 62 Patil, Y.; Ameduri, B. First RAFT/MADIX radical copolymerization of tert-butyl 2-trifluoromethacrylate with vinylidene fluoride controlled by xanthate. *Polymer Chemistry*. **2013**, *4*, 2783-2799.
- 63 Banerjee, S.; M. Wehbi, M.; A. Manseri, A.; , Mehdi, A.; Alaaeddine, A.; Hachem, A.; Ameduri, B. Poly(vinylidene fluoride) containing phosphonic acid as anti-corrosion coating for steel, *ACS Applied Materials & Interfaces*, **2017**, *9*, 6433-6443.
- 64 Wehbi, M.; Banerjee, S.; Mehdi, A.; Alaaeddine, A.; Hachem, A.; Ameduri B. Vinylidene fluoride-based polymer network via cross-linking of pendant triethoxysilane functionality for potential applications in coatings, *Macromolecules* **2017**, *50*, 9329-9339.
- 65 Boujioui, F.; Zhuge, F.; Damerow, H.; Wehbi, M.; Ameduri, B.; Gohy, J.F.. Solid polymer electrolytes from a fluorinated copolymer bearing cyclic carbonate pendant groups, *Journal of Materials Chemistry, A* **2018**, *6*, 8514-8522.

- 66 Guiot, J.; Ameduri, B.; Boutevin, B.; Lannuzel, T. Original crosslinking of poly(vinylidene fluoride) via trialkoxysilane-containing cure-site monomers *Journal of Polymer Science: Part A: Polymer Chemistry*, **2006**, *44*, 3896–3910.
- 67 Guiot, J.; Ameduri, B.; Boutevin, B.; Lannuzel, T. ; Solvay WO2004081066 Fluoromonomères fonctionnalisés et leurs copolymères avec un fluorure de vinylidène. **2004**.
- 68 Ito, H.; Giese, B.; Engelbrecht, R. Radical reactivity and Q-E values of methyl alpha-(trifluoromethyl)acrylate. *Macromolecules* **1984**, *17*, 2204–2205.
- 69 Fedors, R.F. A method of estimating both the solubility parameters and molar volumes of liquids, *Polymer Engineering and Science*, **1974**, *14*, 147-154.
- 70 Gérard, J.F.; Seck, S.; Bounor-Legaré V.; Bigarré, J.; Buvat, P. ; Chauveau J. Procédé de préparation d'un matériau composite échangeur d'ions comprenant une matrice polymère spécifique et une charge consistant en des particules échangeuses d'ions, WO 2014/173885, **2014**.
- 71 Ameduri, B.; Gerard, J.F.; Bounor Legaré,V.; Seck, S.; Buvat, P.; Bigarre, J.; Process for preparing an ion-exchange composite material comprising a polymer matrix and a filler consisting of ion-exchange particles; US20160156052A1 (assigned to CEA, INSA, ENSCM, CNRS)